

Quantum coherence of $1s$ orthoexcitons in Cu_2O driven by resonant two-photon excitation

Shunsuke Kono*

Fundamental and Environmental Research Laboratories, NEC Corporation, 34 Miyukigaoka, Tsukuba, Ibaraki, 301-8501 Japan

Nobukata Nagasawa

Tokyo Instruments, Inc., 6-18-14 Nishikasai, Edogawa-ku, Tokyo, 134-0088 Japan

(Received 4 August 2006; revised manuscript received 23 October 2006; published 22 December 2006)

The intensity of the resonant emission of the $1s$ orthoexcitons in Cu_2O is observed in a weak magnetic field under two-photon resonant excitation at 1.6 K to investigate the quantum interference within the Zeeman sublevels in the Faraday configuration. A specific decrease of $\sim 15\%$ in the emission intensity is observed in the region of ± 0.2 T. This structure is interpreted as a manifestation of the quantum interference effect between the Zeeman sublevels of the $1s$ orthoexcitons, known as the Hanle effect in atomic spectroscopy. The homogeneous width of the exciton level is estimated to be $5.5 \mu\text{eV}$. The contribution of the quadrupole exciton polariton is discussed by taking into account the geometry-dependent characteristics of the exciton-polariton on the direction of the magnetic field. The Hanle structure observed is attributed to the interference of the polariton wave packets of the longitudinal excitons, where the phase coherence is transferred via transverse excitons driven by resonant two-photon coupling with the radiation field.

DOI: [10.1103/PhysRevB.74.245214](https://doi.org/10.1103/PhysRevB.74.245214)

PACS number(s): 71.35.-y, 71.36.+c

I. INTRODUCTION

The Hanle effect, one of the most important phenomena in quantum mechanics, dates back to 1922.¹ Hanle observed that the polarization of the resonant emission of Hg atoms in a weak magnetic field was slightly rotated and depolarized compared with the initial polarization of resonant excitation light. This observation could be classically explained by the damped oscillation of the electronic polarization rotating in a weak magnetic field. The rotation frequency is given by the Larmor frequency. However, Hanle's observation contradicted the classical interpretation. The rotation of the polarization could be interference of the resonant emission from the Zeeman-split levels of the respective atoms. Within the classical treatment, this interference could not happen in a weak magnetic field of as low as 1 G where the phenomenon was observed because the atomic line of the Hg gas was Doppler broadened. Hanle finally explained the phenomenon by taking an idea presented by Bohr into consideration. According to the uncertainty principle, Zeeman sublevels have a natural broadening \hbar/τ , where τ is the lifetime of the excited states. Hanle interpreted his observation on the basis of the fact that the Zeeman sublevels were coherently superposed under a weak magnetic field where the Zeeman splitting was narrower than the homogeneous linewidth. In an experiment on the Hanle effect, the resonant emission observed with a polarizer orthogonal to the initial excitation polarization increases with the magnetic field due to the rotation of the coherently superposed state and then attains to a certain intensity in a strong magnetic field where the Zeeman sublevels are no longer superposed. Thus the intensity of the observed emission as a function of the magnetic field can be fitted with a Lorentzian function whose width gives the homogeneous linewidth of the excited states under investigation.

The Hanle effect is not limited only to for the atomic gases. Similar effects can be observed in any quantum levels being crossed by external fields. This technique is called level crossing spectroscopy. The same kind of the effect for free electrons and holes in semiconductors is known as spin

orientation. For excitons in semiconductors a related phenomenon was first reported by Gross *et al.*² and is known as optical orientation or optical alignment of the exciton spin.³

In the present paper, we report the emission intensity of the $1s$ orthoexcitons of the yellow series in Cu_2O under two-photon resonant excitation in a weak magnetic field, expecting to observe the quantum interference effect on the coherent superposition of the exciton state. The $1s$ orthoexcitons is well known for its quite narrow linewidth and the optical anisotropy inherent in the electric quadrupole coupling to the radiation field.⁴ These peculiarities of its optical interaction have attracted many attentions to investigate the coherent nature of the $1s$ orthoexcitons.

During the past two decades, the coherent properties of the $1s$ orthoexcitons have been mainly studied using time-resolved measurements. Langer *et al.* observed the quantum beat of the Zeeman split-off levels of the $1s$ orthoexcitons in Cu_2O .⁵ The phase relaxation of the coherently superposed states was explained by including the effect of exciton-polariton propagation as one of the relaxation channels. In solid-state materials, the electromagnetic wave couples to the exciton to form a coupled state called the exciton-polariton.⁶ This coupled light-exciton system is a unique characteristic in solid-state materials. The quadrupole exciton-polariton of the relevant exciton state was directly investigated using propagation beat spectroscopy.⁷ Temporal beating of the transmitted light resulted from the group-velocity dispersion of the quadrupole exciton-polariton wave packets. The beating signal also gave the phase relaxation of the exciton-polariton propagation.

In these reports, coherent superposition of the $1s$ orthoexciton was created using coherent excitation with ultrashort laser pulses. The use of time-integrated spectroscopy to measure the Hanle effect is complemented by these kinds of quantum beat spectroscopy methods, where the beating signal is measured in a time-resolved manner.

Previously, we created the $1s$ orthoexciton using band-to-band excitation under a weak magnetic field and observed that the specific structure of the resonant emission intensity

depended on the magnetic field.⁸ According to the symmetry of the Cu_2O crystal, the $1s$ orthoexcitons are triply degenerate. Under a weak magnetic field, a certain combination of the Zeeman sublevels of the $1s$ orthoexciton forms a coherent superposition. We interpreted this observed structure as a manifestation of the Hanle effect of the $1s$ orthoexcitons in Cu_2O . The width of the structure was estimated to be $8.8 \mu\text{eV}$, and this value was interpreted as the homogeneous linewidth of the $1s$ orthoexciton.

In the previous report, no specific polarization was created as a result of band-to-band excitation. However, a specific polarization component was observed by selecting the wave vector and polarization of the observation according to the electric quadrupole interaction. In the present paper, we expand on the previous observation of the Hanle effect of the $1s$ orthoexcitons in Cu_2O by using resonant two-photon excitation in Faraday geometry. According to the parity-conserving characteristics of the band structure, the $1s$ orthoexcitons are allowed for the electric-dipole two-photon transition. Resonant two-photon excitation enables us to create a specific polarization of the relevant exciton. Thus, compared to the case of band-to-band excitation, the present experimental condition described here is closer to that of Hanle's original experiment, where the specific polarization of the Hg atoms was resonantly created.

Furthermore, the specific polarization of the relevant exciton created by resonant two-photon excitation will have a finite wave vector defined by the dispersion of the quadrupole exciton polariton. As has been pointed out previously in Refs. 5 and 7, the propagation characteristics of the quadrupole exciton polariton play an important role in the coherent properties of the $1s$ orthoexcitons in Cu_2O . Moskalenko and Liberman treated our previous observation of the Hanle effect of the $1s$ orthoexcitons as the time-integrated measurement of the interference effect of the exciton-polariton wave packets.⁹

In this article, we discuss the magnetic field dependence of the resonant emission of the $1s$ orthoexciton in different geometries based on exciton-polariton propagation. In Sec. II, the Zeeman sublevels of the $1s$ orthoexcitons are explained in different geometries of the magnetic field in order to compare our present and previous measurements. The experimental condition is briefly described in Sec. III, and in Sec. IV, the results are discussed based on the propagation effects of the quadrupole exciton polariton.

II. $1s$ ORTHOEXCITON IN A MAGNETIC FIELD

The triply degenerate $1s$ orthoexciton in Cu_2O is represented by the irreducible representation of Γ_5^+ in the point group of O_h symmetry. We denote the base functions of this representation as $|x\rangle$, $|y\rangle$, and $|z\rangle$, which are represented by the functional forms of yz , zx , and xy , respectively. Under Voigt geometry, where the wave vector of the observed emission and direction of the external magnetic field are, respectively, parallel to the $[001]$ and $[100]$ directions, the split-off Zeeman levels are described with the base functions of the orthoexciton as follows:¹⁰

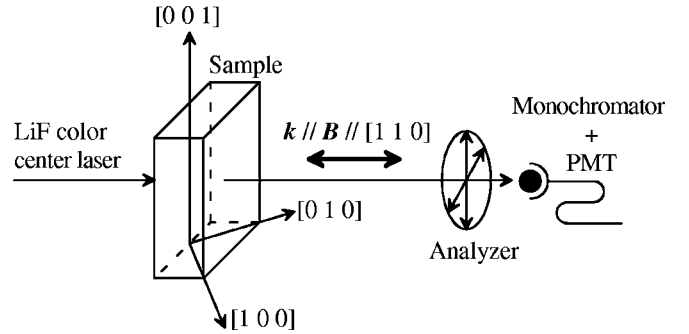


FIG. 1. Schematic representation of the experimental geometry of the Cu_2O crystal.

$$|m = +1\rangle = \frac{1}{\sqrt{2}}(|y\rangle + i|z\rangle),$$

$$|m = 0\rangle = |x\rangle,$$

$$|m = -1\rangle = \frac{1}{\sqrt{2}}(|y\rangle - i|z\rangle). \quad (1)$$

The electric quadrupole interaction allows only the $|m = \pm 1\rangle$ Zeeman states to couple with the $[100]$ -polarized light field. On the other hand, the $|m = 0\rangle$ state couples with the $[010]$ -polarized light field in the same interaction. In our previous paper, a specific magnetic field dependence of the time-integrated emission was observed around zero magnetic fields with the $[100]$ -polarized analyzer because the sublevels of $|m = \pm 1\rangle$ were coherently superposed.

A recent investigation of the $1s$ orthoexciton using ultra high-resolution spectroscopy has revealed the inherent splitting of the $1s$ orthoexciton state due to the wave-vector-dependent exchange interaction.^{11–13} When the wave vector is parallel to the $[001]$ direction, as in our previous paper, the interaction Hamiltonian of the exchange interaction has only diagonal components that do not mix the base functions of the $1s$ orthoexcitons under O_h symmetry. Thus, the Hanle dip observed in our previous paper is concluded to be the interference of the Zeeman sublevels in Eq. (1).

In the present paper, we treat resonant two-photon excitation of the $1s$ orthoexciton state in Faraday geometry, where the wave vector of the incident laser, external magnetic field, and direction of the observation are parallel to the $[110]$ direction.

Figure 1 shows a schematic representation of the present experimental configuration. In this geometry, where $\mathbf{k} \parallel [110]$, the wave-vector-dependent exchange interaction mixes the base functions of the $1s$ orthoexcitons. The Zeeman energy discussed in this paper is comparable to the wave-vector-dependent exchange interaction. Therefore, the interaction Hamiltonian including both the Zeeman effect and wave-vector-dependent exchange interaction has to be simultaneously diagonalized. After this simultaneous diagonalization, we obtained the split-off levels of the $1s$ orthoexciton described by the original base functions of Γ_5^+ :

$$\begin{aligned}
 |m = +1\rangle &= \frac{1}{\sqrt{2\alpha_{+1}^2 + 1}} [i\alpha_{+1}(|x\rangle - |y\rangle) + |z\rangle], \\
 |m = 0\rangle &= \frac{1}{\sqrt{2}} (|x\rangle + |y\rangle), \\
 |m = -1\rangle &= \frac{1}{\sqrt{2\alpha_{-1}^2 + 1}} [i\alpha_{-1}(|x\rangle - |y\rangle) + |z\rangle]. \quad (2)
 \end{aligned}$$

The diagonalization of the interaction Hamiltonian is given in the Appendix. Here, the coefficients $\alpha_{\pm 1}$ represent the mixing between the states $|x\rangle - |y\rangle$ and $|z\rangle$ due to the magnetic field. According to the respective coefficients of the base functions, the Zeeman sublevels of $|m = \pm 1\rangle$ are transverse and the sublevel of $|m = 0\rangle$ is longitudinal. In this geometry, the $|z\rangle$ components of the excitons of $|m = \pm 1\rangle$ are allowed for the electric-dipole two-photon transition with a linearly polarized light parallel to $[1\bar{1}0]$, while the sublevel of $|m = 0\rangle$ is allowed for quadrupole one-photon transition with a linearly polarized light parallel to the $[001]$ direction. Thus, a coherent superposition of the $|m = \pm 1\rangle$ states should be formed by two-photon resonant excitation in a weak magnetic field because the spectral width of the excitation light was broader than the wave-vector-dependent exchange splitting at zero magnetic field. The intensity of the resonant emission from the $|m = 0\rangle$ state with the analyzer parallel to $[001]$ is expected to show specific magnetic field dependence as a manifestation of the Hanle effect because the quantum interference effect between the $|m = \pm 1\rangle$ states should be reflected in this one-photon resonant emission. When the magnetic field approaches zero, the coefficient α_{+1} increases to infinity and α_{-1} vanishes, so that sublevels due to the wave-vector-dependent exchange interaction are obtained. On the other hand, when the Zeeman energy is much larger than the wave-vector-dependent exchange splitting, the ratio $\alpha_{\pm 1}$ approaches $\pm 1/\sqrt{2}$. In this case, the sublevels are approximately given by diagonalization of the interaction Hamiltonian only with consideration of the Zeeman effect.

III. EXPERIMENT

A single crystal of $2 \times 2 \times 4 \text{ mm}^3$ cut from a naturally grown Cu_2O crystal was used as our sample. The sample was irradiated with a LiF color center laser (Solar CF-151M) pumped with a Q -switched Nd:YAG laser (Quantronix A532 O/QS). The spectral width and repetition rate of the light source were 0.05 meV and 1 kHz, respectively. The pulse duration was about 20 ns. The resonant emission was dispersed by a 2-m single monochromator and was detected by a photomultiplier (Hamamatsu R-955). The polarization of the resonant emission was analyzed by rotating a Polaroid-sheet-type polarizer before the entrance slit of the monochromator. The polarization angle of the incident laser was tuned by rotating a half-wave plate around the excitation optical axis. A split-type superconducting magnet (CRYO Industries, Model SM6) was used for magneto-optical measurements. The measurements were performed at 1.6 K.

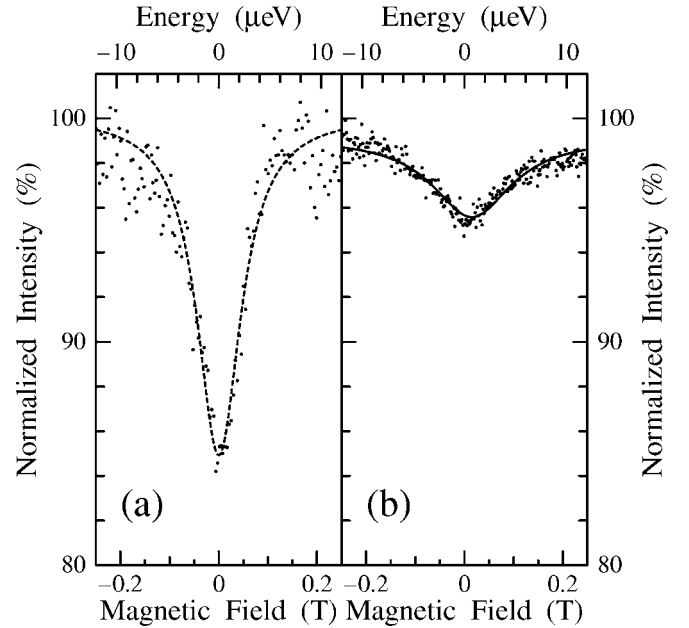


FIG. 2. (a) Integrated intensity of the resonant emission from the state $|m=0\rangle$ as a function of the external magnetic field in Faraday geometry under two-photon resonant excitation. Dashed curve represents best-fitted curve giving 2γ to be $5.5 \mu\text{eV}$. (b) Integrated intensity of resonant emission from the states $|m = \pm 1\rangle$ as a function of the external magnetic field in Voigt geometry under band-to-band excitation (Ref. 8). Solid curve represents best-fitted curve giving 2γ to be $8.8 \mu\text{eV}$.

IV. RESULTS AND DISCUSSION

Figure 2(a) shows the integrated intensity of the resonant emission of the $|m=0\rangle$ state under two-photon resonant excitation as a function of the external magnetic field. A remarkable decrease in emission intensity was observed around zero magnetic field. In this figure, the magnetic field dependence is normalized by the spectrum of the second harmonic of the incident laser whose center wavelength was at the $1s$ orthoexciton energy without a magnetic field. The two-photon energy of the excitation light fully covered the resonance of the $1s$ orthoexciton. The width of this exciton state is estimated by the following Lorentz function given in Ref. 14:

$$I \propto \frac{1}{\gamma} - \frac{\gamma}{\gamma^2 + \omega_L^2} + (\text{background}). \quad (3)$$

Here, ω_L is the Larmor frequency of the $1s$ orthoexciton given by $\omega_L = g_F \mu_B B / 2$. We determined g_F to be 1.66 estimated from the Zeeman splitting in large magnetic fields.¹⁵ The dashed curve in Fig. 2(a) represents the best-fitted curve giving 2γ as $5.5 \mu\text{eV}$.

The homogeneous linewidth estimated in this work is smaller than that in the previous work. To compare them, we reproduced the previous measurement of the magnetic field dependence of the resonant emission in Fig. 2(b).⁸ The linewidth previously estimated using the above formula, shown by the solid curve, was $8.8 \mu\text{eV}$, which is larger than the corresponding value estimated in this paper. The depth of the

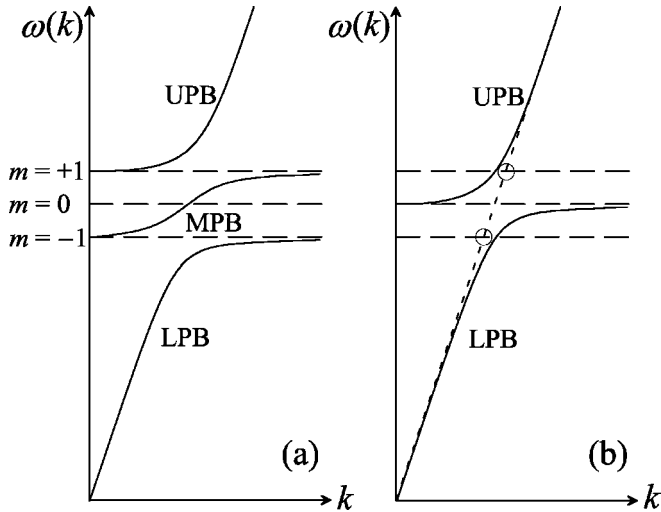


FIG. 3. (a) Solid curves represent quadrupole exciton-polariton dispersion with [100]-polarized light field in Voigt geometry ($\mathbf{k}\parallel[001]$, $\mathbf{B}\parallel[100]$). (b) Quadrupole exciton-polariton dispersion with [010]-polarized light field in Voigt geometry ($\mathbf{k}\parallel[001]$, $\mathbf{B}\parallel[100]$). This dispersion is equivalent to that in Faraday geometry where $\mathbf{k}\parallel\mathbf{B}\parallel[110]$ with light polarization parallel to [001] (Ref. 16).

observed structure is also deeper than that of the previously observed one. These differences are explored below.

We discuss the difference in the homogeneous linewidth between our present and previous results including the effect of exciton-polariton propagation. Moskaleiko and Liberman developed a theory of the Hanle effect on excitons in semiconductors that took account of the effect of polariton propagation based on our previous measurement of the Hanle effect of the $1s$ orthoexcitons.⁹ The resonant emission of the $1s$ orthoexciton is emitted from the crystal after the exciton polariton propagates through it. Around the resonance of the quadrupole exciton polariton, Moskaleiko and Liberman treated two wave packets of the same group velocity, one on the upper and the other on the lower polariton branch, to investigate the interference between them. The condition of the interference between the two wave packets depends on their phase coherence. During propagation, the polariton may be scattered by acoustic phonons. This scattering is characterized by the damping constant $2\gamma=1/\tau_{coh}$. To observe the time-integrated interference effects of the two wave packets on the polariton branches, the traveling time of the exciton polariton through the crystal should be shorter than the coherence time of the exciton polariton, τ_{coh} . We have previously noted the influence of polariton effects on these phenomena.^{8,16}

In the previous geometry, the [100]-polarized light field and the $|m=\pm 1\rangle$ states of Eq. (1) form three polariton branches in Fig. 3(a): (Refs. 8 and 9) the upper polariton branch (UPB) from $|m=+1\rangle$, lower polariton branch (LPB) from $|m=-1\rangle$, and middle polariton branch (MPB) connecting between $|m=+1\rangle$ and $|m=-1\rangle$. Wave packets propagating faster than τ_{coh} are on the UPB and LPB because the group velocity of the MPB is extremely slow compared with the light velocity. The peculiar structure observed around the zero magnetic field is mainly due to the energy separation

between the UPB and LPB given by Eq. (62) in Ref. 9. This energy separation is proportional to the Zeeman splitting, $2\hbar\omega_L$.

In contrast to the case of the resonant emission from the $|m=\pm 1\rangle$ states, the resonant emission from the $|m=0\rangle$ state did not show any specific structure around the zero magnetic field as shown in Fig. 2 of Ref. 8. This is due to the fact that the exciton-polariton dispersion of the $|m=0\rangle$ state is not affected by the magnetic field as shown in Fig. 3(b), which illustrates the formation of an exciton polariton.

In the present experiment, the specific structure observed with the resonant emission of the $|m=0\rangle$ state can be also explained by the interference of the polariton wave packets on the UPB and LPB of the $|m=0\rangle$ state. These wave packets could be, respectively, converted from excitons of the $|m=\pm 1\rangle$ states created by two-photon resonant excitation. In a weak magnetic field, where $|m=\pm 1\rangle$ were coherently superposed, the phase of the superposed state is transferred to the wave packets on these polariton branches. Thus, the increasing emission intensity can be explained by the increase in the group velocity of the wave packets whose frequencies were at the Zeeman split-off states of $|m=\pm 1\rangle$, though the exciton-polariton dispersion of $|m=0\rangle$ does not depend on the magnetic field. The narrower width of the observed Hanle structure compared to the previous measurement is due to the fact that the exciton-polariton dispersion of $|m=0\rangle$ state does not depend on the magnetic field.

At the moment of conversion from the $|m=+1\rangle$ ($|m=-1\rangle$) exciton to the wave packet on the UPB (LPB), however, the mismatch of the wave vector should be considered because the exciton-polariton dispersion and two-photon light dispersion do not overlap around the resonance of the $1s$ orthoexciton. The excitons created by the resonant two-photon excitation correspond to the circles in Fig. 3(b). The mismatch of the wave vector may be compensated for by the acoustic phonon scattering. Other than scattering during polariton propagation, acoustic phonon scattering may degrade the phase coherence of the $|m=\pm 1\rangle$ states that provide an initial phase for the interference of the two wave packets. The spreading out of the initial phase of the wave packets may not be as large because the splitting of the quadrupole exciton polariton is quite small and the sound velocity of the acoustic phonons is much less than the light velocity in the crystal.

The difference in the ratio of the observed Hanle dip to the emission intensity at zero magnetic fields seen in Figs. 2(a) and 2(b) can be also explained by taking the exciton-polariton propagation into account.¹⁹ Both Figs. 2(a) and 2(b) are normalized with the emission intensity in the large-magnetic-field regime, where $\hbar\omega_L \gg 2\gamma$. The dip in the structure in Fig. 2(a) is deeper than that in Fig. 2(b). This suggests that the phase coherence of the superposed state is better in the case of resonant two-photon excitation than that of band-to-band excitation. In the case of band-to-band excitation, the exciton polaritons were formed after the kinetic relaxation of the electron-hole pairs with excess energy. Furthermore, the propagation distance of exciton polaritons will be restricted close to the crystal surface due to the absorption of the excitation laser. Thus, the background emission at zero magnetic fields was attributed to luminescence and a quite

small portion of the exciton-polariton keeping the phase coherence contributed to the Hanle structure.

In the case of resonant two-photon excitation, the propagation distance was the entire thickness of the crystal.²⁰ With this picture of polariton propagation, it is possible to give a quantitative estimate of the ratio of the Hanle structure to the background emission. The linewidth estimated in this paper, $5.5 \mu\text{eV}$, gives the coherence time of the exciton-polariton wave packet, estimated to be 240 ps. The thickness of the sample gives the minimum group velocity of the exciton polariton that can escape from the sample. This minimum group velocity is estimated to be $v_{gm}=8.3 \times 10^6$ m/s. According to the group velocity dispersion relation calculated in Fig. 2(b) in Ref. 7, an exciton polariton slower than v_{gm} is within $\pm 16 \mu\text{eV}$ of the exciton resonance. In the present experiment, an exciton polariton faster than v_{gm} may have contributed to the background emission other than the Hanle structure. The linewidth of the excitation laser at two-photon energy was about $100 \mu\text{eV}$. Therefore, the ratio of the exciton-polariton slower than v_{gm} can be estimated to be about $1/3 \sim 32 \mu\text{eV}/100 \mu\text{eV}$. This ratio is close to the depth of the observed Hanle dip against the total emission intensity in Fig. 2(a). The observation of a Hanle structure shallower than the estimated ratio may be due to the phase degradation at the moment of the conversion from the $|m = \pm 1\rangle$ excitons to the wave packets on the $|m=0\rangle$ exciton-polariton branches.

The linewidth observed in the present report is larger than the recently reported linewidth measured using ultrahigh-resolution spectroscopy.^{11–13} Due to wave-vector-dependent exchange splitting of the $1s$ orthoexciton, the Zeeman splitting energy was not linear to the magnetic field, where the Zeeman energy was comparable to this inherent splitting. Thus, the estimated linewidth in this report can be offset by the energy splitting at zero magnetic field. The energy splitting of $|m = \pm 1\rangle$ at zero magnetic field is $4.2 \mu\text{eV}$.^{11–13} Thus, the energy shift due only to the Zeeman effect is estimated to be $1.3 \mu\text{eV}$, which is closer to the latest reported value. However, this value is still larger than the reported one. One of the reasons for the broader linewidth may be internal strain, which can be explained as follows. The sublevels $|m = \pm 1\rangle$ were not split due to the wave-vector-dependent exchange splitting in Voigt geometry, where we previously reported the linewidth of $8.8 \mu\text{eV}$. This larger value was due to band-to-band excitation because the polariton propagation was restricted to the shallow depth of the sample surface, where internal strain could have a significant effect.¹³

In reports of the observation of resonant second-harmonic scattering and hyper-Raman scattering via the $1s$ orthoexcitons in Cu_2O , resonant luminescence of the relevant excitons was also observed.^{17,18} In these observations of resonant light scattering, the phase coherence of the excited states was one of the criteria used to distinguish the coherent scattering part from the luminescence part. One of the experimental methods used to extract the coherent part of the resonant emission was the time-resolved quantum beat spectroscopy as mentioned in the report of Langer *et al.*⁵ The contrast of the Hanle structure estimated in our discussion considering the effects of polariton propagation corresponds to the luminescence part of the resonant emission in the present two-photon

resonant excitation. The resonant light scattering of the relevant exciton state can be consistently explained by our time-integrated observation according to the propagation of the polariton wave packets.

V. CONCLUSIONS

We observed the resonant emission of the $1s$ orthoexcitons in Cu_2O under two-photon resonant excitation in a weak magnetic field. We interpreted the specific structure of the emission intensity dependent on the magnetic field as quantum interference of the Zeeman split-off states—the so-called Hanle effect in atomic spectroscopy. The homogeneous line width was estimated to be $5.5 \mu\text{eV}$. We compared this estimated value with the previously reported homogeneous linewidth taking into account the effect of exciton-polariton propagation. The proportion of the observed Hanle structure to the background emission was explained by the acoustic phonon scattering of the propagating exciton-polariton wave packets.

ACKNOWLEDGMENTS

The authors acknowledge N. Naka for her helpful discussion. The authors acknowledge S. A. Moskalenko and M. A. Liberman for paying attention to our previous work and for providing a copy of their paper⁹ in advance of publication.

APPENDIX: SUBLEVELS OF $1s$ ORTHOEXCITONS UNDER ZEEMAN EFFECT AND WAVE-VECTOR-DEPENDENT EXCHANGE INTERACTION

In the present paper, the case of $\mathbf{k} \parallel \mathbf{B} \parallel [110]$ is considered. According to Ref. 13, the long-range quadrupole-quadrupole exchange Hamiltonian is given by the following matrix with $(k_x, k_y, k_z) = \frac{1}{\sqrt{2}}(1, 1, 0)$:

$$\mathbf{J}_{ex}^Q = \Delta_Q \begin{pmatrix} 0 & 0 & 0 \\ 0 & 0 & 0 \\ 0 & 0 & 1/4 \end{pmatrix}. \quad (\text{A1})$$

With the same wave vector, the short-range exchange interaction Hamiltonian with nonvanishing components is given by the following matrices:

$$\mathbf{J}_3 = \Delta_3 \begin{pmatrix} 1/2 & 0 & 0 \\ 0 & 1/2 & 0 \\ 0 & 0 & -1 \end{pmatrix}, \quad (\text{A2})$$

$$\mathbf{J}_5 = \Delta_5 \begin{pmatrix} 0 & 1/2 & 0 \\ 1/2 & 0 & 0 \\ 0 & 0 & 0 \end{pmatrix}. \quad (\text{A3})$$

The interaction Hamiltonian attributed to the wave-vector-dependent exchange interaction is given as the sum of the above three matrices:

$$\mathbf{H}_{ex} = \mathbf{J}_{ex}^Q + \mathbf{J}_3 + \mathbf{J}_5 \quad (\text{A4})$$

$$= \begin{pmatrix} \frac{\Delta_3}{2} & \frac{\Delta_5}{2} & 0 \\ \frac{\Delta_5}{2} & \frac{\Delta_3}{2} & 0 \\ 0 & 0 & \frac{\Delta_Q}{4} - \Delta_3 \end{pmatrix}. \quad (\text{A5})$$

The magnetic field is represented by the Γ_4^+ irreducible representation under the O_h group. The interaction Hamiltonian by the magnetic field is given by the following matrix with the magnetic field $(B_x, B_y, B_z) = \frac{1}{2}(1, 1, 0)$:

$$\mathbf{H}_B = \frac{\mu_B g_F B}{\sqrt{2}} \begin{pmatrix} 0 & 0 & i \\ 0 & 0 & -i \\ -i & i & 0 \end{pmatrix}. \quad (\text{A6})$$

Here, μ_B is the Bohr magneton and g is the exciton g factor. The total interaction Hamiltonian including the Zeeman effect and wave-vector-dependent exchange interaction is given by the following equation:

$$\mathbf{H}_{int} = \mathbf{H}_{exch} + \mathbf{H}_B. \quad (\text{A7})$$

The diagonalization of the Hamiltonian \mathbf{H}_{int} provides us with the sublevels of the $1s$ orthoexcitons. The sublevels are described by the following equations:

$$|m = +1\rangle = \frac{1}{\sqrt{2\alpha_{+1}^2 + 1}} [i\alpha_{+1}(|x\rangle - |y\rangle) + |z\rangle], \quad (\text{A8})$$

$$|m = 0\rangle = \frac{1}{\sqrt{2}}(|x\rangle + |y\rangle), \quad (\text{A9})$$

$$|m = -1\rangle = \frac{1}{\sqrt{2\alpha_{-1}^2 + 1}} [i\alpha_{-1}(|x\rangle - |y\rangle) + |z\rangle]. \quad (\text{A10})$$

Here, $\alpha_{\pm 1}$ are the parameters mixing the states $|x\rangle - |y\rangle$ and $|z\rangle$. By diagonalization, $\alpha_{\pm 1}$ are obtained as the following equations:

$$\alpha_{+1} = - \frac{\left(\frac{g\mu_B B}{\sqrt{2}}\right)^2 + \frac{\Delta_5}{2} \left(\frac{\Delta_Q}{4} - \Delta_3 - \epsilon_{+1}\right)}{\frac{g\mu_B B}{\sqrt{2}} \left(\frac{\Delta_3}{2} - \frac{\Delta_5}{2} - \epsilon_{+1}\right)}, \quad (\text{A11})$$

$$\alpha_{-1} = - \frac{\left(\frac{g\mu_B B}{\sqrt{2}}\right)^2 + \frac{\Delta_5}{2} \left(\frac{\Delta_Q}{4} - \Delta_3 - \epsilon_{-1}\right)}{\frac{g\mu_B B}{\sqrt{2}} \left(\frac{\Delta_3}{2} - \frac{\Delta_5}{2} - \epsilon_{-1}\right)}. \quad (\text{A12})$$

The eigenenergies denoted by $\epsilon_{\pm 1}$ and ϵ_0 are, respectively, given by the eigenvalues of the interaction Hamiltonian \mathbf{H}_{int} :

$$\epsilon_0 = \frac{1}{2}(\Delta_3 + \Delta_5), \quad (\text{A13})$$

$$\epsilon_{+1} = \frac{1}{2} \left[-\frac{\Delta_3}{2} - \frac{\Delta_5}{2} + \frac{\Delta_Q}{4} + \sqrt{\left(\frac{3}{2}\Delta_3 - \frac{\Delta_5}{2} - \frac{\Delta_Q}{4}\right)^2 + 8\left(\frac{g\mu_B B}{\sqrt{2}}\right)^2} \right], \quad (\text{A14})$$

$$\epsilon_{-1} = \frac{1}{2} \left[-\frac{\Delta_3}{2} - \frac{\Delta_5}{2} + \frac{\Delta_Q}{4} - \sqrt{\left(\frac{3}{2}\Delta_3 - \frac{\Delta_5}{2} - \frac{\Delta_Q}{4}\right)^2 + 8\left(\frac{g\mu_B B}{\sqrt{2}}\right)^2} \right]. \quad (\text{A15})$$

When the Zeeman energy is much larger than the wave-vector-exchange splitting, the sublevels described by Eqs. (A8)–(A10) are, respectively, approximated by the following equations:

$$|m = +1\rangle \approx \frac{1}{\sqrt{2}} \left[\frac{i}{\sqrt{2}}(|x\rangle - |y\rangle) + |z\rangle \right], \quad (\text{A16})$$

$$|m = 0\rangle \approx \frac{1}{\sqrt{2}}(|x\rangle + |y\rangle), \quad (\text{A17})$$

$$|m = -1\rangle \approx \frac{1}{\sqrt{2}} \left[-\frac{i}{\sqrt{2}}(|x\rangle - |y\rangle) + |z\rangle \right]. \quad (\text{A18})$$

At the other extreme, when the magnetic field approaches zero, the level is split only by the wave-vector-dependent exchange interaction. The sublevels are described by the following wave functions: $\frac{1}{2}(|x\rangle - |y\rangle)$, $\frac{1}{2}(|x\rangle + |y\rangle)$, $|z\rangle$.

*Electronic address: s-kono@cq.jp.nec.com

¹W. Hanle, Zs. Fys. **30**, 93 (1924).

²E. F. Gross, E. I. Ekimov, B. S. Razbirin, and V. I. Safarov, Zh. Eksp. Teor. Fiz. Pis'ma Red. **14**, 108 (1971).

³G. E. Pikus and E. L. Ivchenko, *Excitons* (North-Holland, Amsterdam, 1982), Chap. 6.

⁴R. J. Elliott, Phys. Rev. **124**, 340 (1961).

⁵V. Langer, H. Stolz, and W. von der Osten, Phys. Rev. B **51**, 2103 (1995).

⁶J. J. Hopfield, Phys. Rev. **112**, 1555 (1958).

⁷D. Fröhlich, A. Kulik, B. Uebbing, A. Mysyrowicz, V. Langer, H. Stolz, and W. von der Osten, Phys. Rev. Lett. **67**, 2343 (1991).

⁸S. Kono and N. Nagasawa, Solid State Commun. **110**, 159 (1999).

⁹S. A. Moskalenko and M. A. Liberman, Phys. Rev. B **65**, 064303 (2002).

¹⁰G. F. Koster, J. O. Dimmock, R. G. Wheeler, and H. Statz, *Properties of Thirty-Two Point Groups* (MIT Press, Cambridge, MA, 1963).

¹¹G. Dasbach, D. Fröhlich, H. Stolz, R. Klieber, D. Suter, and M. Bayer, Phys. Rev. Lett. **91**, 107401 (2003).

¹²G. Dasbach, D. Fröhlich, H. Stolz, R. Klieber, D. Suter, and M. Bayer, Phys. Status Solidi B **238**, 541 (2003).

¹³G. Dasbach, D. Fröhlich, R. Klieber, D. Suter, M. Bayer, and H.

- Stolz, Phys. Rev. B **70**, 045206 (2004).
- ¹⁴G. Moruzzi and F. Strumia, *The Hanle Effect and Level-Crossing Spectroscopy* (Plenum, New York, 1991).
- ¹⁵S. Kono and N. Nagasawa, Solid State Commun. **110**, 93 (1999).
- ¹⁶S. Kono, Ph.D. thesis, University of Tokyo, 1999.
- ¹⁷S. Kono, N. Naka, M. Hasuo, S. Saito, T. Suemoto, and N. Nagasawa, Solid State Commun. **97**, 455 (1996).
- ¹⁸M. Y. Shen, S. Koyama, M. Saito, T. Goto, and N. Kuroda, Phys. Rev. B **53**, 13477 (1996).
- ¹⁹In Fig. 2 of Ref. 8, we did not scale the signal from the zero level because the analysis was focused on the width of the Hanle structure. In the present paper, the emission signals are scaled from the zero level to show the difference seen in the respective excitation conditions.
- ²⁰Moskalenko and Liberman analyzed the results of Ref. 8 with a crystal thickness of 5 mm (Ref. 9). However, the actual thickness of the sample was 2 mm because the explanation of the sample orientation in Ref. 8 was misleading.